

# A Robust Torque Control Approach for Gear Shift of a Parallel Hybrid Electric Vehicle with Dual Clutch Transmission

Sooyoung Kim<sup>a)</sup> Seibum Choi<sup>b)</sup>

**This paper proposes a robust control strategy for gear shifts of a parallel-type hybrid electric vehicle (HEV) equipped with a dry dual clutch transmission (DCT). A vehicle equipped with DCT requires accurate torque transfer control through the driveline during gear shifts to ensure good shift quality in the absence of smoothing effects from torque converter. Unlike conventional vehicles driven only by internal combustion engines, a HEV can utilize the drive motor to improve its gear shifting performances. In this paper, an integrated torque and speed control strategy is developed to minimize the driveline oscillations that occur during gear shifts and to complete the shift as fast as the driver wants. A robust H-infinity controller is designed to control transmission output torque as well as clutch slip speed, particularly in inertia phase that mostly determines the total shift quality. The effectiveness of the proposed control strategy as well as its robustness is verified by comparative studies using a proven vehicle model developed in MATLAB/SimDriveline.**

Primary subject classification: 49; Secondary subject classification: 76

## 1 INTRODUCTION

Hybrid electric vehicles (HEVs) use dual energy sources, a fuel and electrical energy, effectively to provide better fuel economy and lower emissions than conventional engine-driven vehicles. In order to improve the performance of the HEV, it is important to manage the power distribution between the two sources and determine the optimum gear ratio under all driving conditions. The general purpose of such power management control strategy is to minimize fuel consumption while meeting other constraints such as the driver's power demand and drivability, emissions, and regulation of state of charge. Previously, several power management strategies have been proposed to optimize the fuel economy and emissions of HEVs in various configurations<sup>1-3</sup>. Power management control provides set-points for individual servo control loops operating at much higher frequencies. To achieve the optimized HEV performance designed by power management strategies, each servo control loop must achieve its set-point reliably through practical control algorithms that take into account characteristics of real hardware or actuators. Control of the transmission system is particularly important to carry out the actual gear shifting for the optimal gear commanded by the power management control loop. In order to achieve the best fuel economy during gear shifting, the optimal gear ratio must be achieved as quickly as possible by minimizing the shift transient time. However, if the gear shift is carried out too quickly, large torque vibrations may occur through the driveline, which may result in poor shifting quality. Thus, the objective of the gear shift control is to achieve both smooth and fast shift performances.

This research copes with gear shift control of a parallel-type HEV with a dry dual-clutch transmission (DCT). The structure of the HEV driveline with a DCT is briefly illustrated in Fig. 1. The integrated starter generator (ISG) used for engine start is connected to the engine via a belt.

a) Transmission Control Development Team, Hyundai Motor Company, Hwasung 18280; sooyoung@hyundai.com.

b) Department of Mechanical Engineering, KAIST, Daejeon 34141, Korea; sbchoi@kaist.ac.kr.

The engine clutch is used when the mode change from pure electric vehicle mode to parallel hybrid mode is required. DCTs use two sets of clutches and transfer shafts during gear shifting to transfer the torque transmitted by power source to the wheel without using a torque converter, effectively overcoming the disadvantages of other types of transmissions. However, since there is no smoothing effect of torque converters, DCT powertrains can cause awkward shifting shocks, especially when the shifting is performed swiftly<sup>4, 5</sup>. In general, smooth and fast shifting conditions collide with each other and are generally considered as two main goals of shift control<sup>6</sup>. Though the clutch-to-clutch shifting process is similar to that of ATs, DCTs where the torque converter is absent require more elaborate control of clutches and power sources focusing on shift shock minimization<sup>7, 8</sup>. In this paper, a novel torque and speed control strategy is proposed to improve the gear shift performance of a parallel HEV with DCT. This study seeks to achieve the desired shift performance by simultaneous tracking control of dynamic output torque and speed states during the shift transient. In addition, a robust multivariable controller is designed to handle the model uncertainties and unknown disturbances effectively. This work focuses particularly on the robustness analysis of the proposed control scheme.

This paper is organized as follows. In Sec. 2, a control-oriented driveline model for a parallel HEV with dry DCT is introduced. Also, the detailed design procedure of the robust gear shift controller is described. In Sec. 3, the robustness and the tracking performance of the proposed gear shift controller are demonstrated through comparative studies. Finally, this work is concluded in Sec. 4.

## 2 MODELING AND CONTROLLER DESIGN

A gear shift process of DCTs is discriminated as torque phase where the torque handover from the off-going clutch to the on-coming one is performed and inertia phase where the speed of the power sources is synchronized with the input shaft speed with a new gear ratio. Since the shift quality is dominantly determined in the inertia phase where the inertial effects of the power sources cause large driveline oscillations, many previous studies focused on the inertia phase control to improve the shifting performances<sup>9-11</sup>. This research also developed an effective control method for the inertia phase of the HEV with DCT. The speed change of the power sources during the inertia phase produces large overshoot of the output shaft torque, which leads to poor ride quality. The regenerative operation of the drive motor can be used for the inertia torque compensation, which also improves fuel economy. In this paper, an integrated torque and speed control approach is proposed such that the shift control problem is interpreted as the torque and speed tracking problem. Given the reference value trajectories of the slip speed and the output torque satisfying the desired shift performances, an effective controller is required to track them accurately. To ensure accurate tracking control of both control states, a robust controller based on H-infinity loop shaping will be designed in the next subsections.

### 1 System Modeling

Because this study copes with gear shift control of a HEV, its parallel mode operations are only considered where the vehicle is partially or fully driven by the engine with the engine clutch fully engaged. The control model needs to be simplified to be implemented for automotive control applications. Considering that the gear shift of the DCT is performed through the torque transfer from one clutch to the other clutch in the driveline, i.e. a clutch-to-clutch shift, a reduced driveline model

that focuses on the clutch-to-clutch shift procedure should be implemented. Another structural requirement of the control-oriented model is that the model should describe the behavior of the driveline system as accurately as possible by using already available information in production cars. The 3<sup>rd</sup> order reduced driveline model for the controller design is described as (1)<sup>12</sup>.

$$\begin{aligned} \dot{\mathbf{x}} &= \mathbf{A}\mathbf{x} + \mathbf{B}\mathbf{u} + \mathbf{E}\delta \quad \text{where} \\ \mathbf{x} &= (x_1, x_2, x_3), \quad \mathbf{u} = (T_m, T_{c1}, T_{c2}), \quad \delta = T_v \\ \mathbf{A} &= \begin{bmatrix} 0 & 0 & \frac{1}{J_{a2,eq}} \\ 0 & 0 & -\left(\frac{1}{i_{12}i_{f2}J_{a2,eq}} + \frac{1}{J_v}\right) \\ 0 & k_o & -c_o\left(\frac{1}{i_{12}i_{f2}J_{a2,eq}} + \frac{1}{J_v}\right) \end{bmatrix}, \mathbf{E} = \begin{bmatrix} 0 \\ \frac{1}{J_v} \\ \frac{c_o}{J_v} \end{bmatrix} \\ \mathbf{B} &= \begin{bmatrix} \frac{1}{J_m} & -\left(\frac{1}{J_m} + \frac{i_{11}i_{f1}}{J_{a2,eq}}\right) & -\left(\frac{1}{J_m} + \frac{i_{12}i_{f2}}{J_{a2,eq}}\right) \\ 0 & \frac{i_{11}i_{f1}}{i_{12}i_{f2}J_{a2,eq}} & \frac{1}{J_{a2,eq}} \\ 0 & \frac{c_o i_{11}i_{f1}}{i_{12}i_{f2}J_{a2,eq}} & \frac{c_o}{J_{a2,eq}} \end{bmatrix} \end{aligned} \quad (1)$$

where:

- $\dot{\phi}_2$  = slip speed between the drive motor and the oncoming clutch (clutch 2), rad/s
- $\dot{\phi}_v$  = torsional compliance rate through the output shaft, rad/s
- $T_v$  = output shaft torque, N·m
- $J_m$  = equivalent inertia of the power sources side, kg·m<sup>2</sup>
- $J_{a2,eq}$  = equivalent inertia of the transmission part seen from the output shaft that includes the inertias of all the components rotating synchronously with the input shaft 2, kg·m<sup>2</sup>
- $J_v$  = vehicle inertia, kg·m<sup>2</sup>
- $i_{11}$  = gear ratio of the input and transfer shaft 1
- $i_{f1}$  = final reduction gear ratio 1
- $i_{12}$  = gear ratio of the input and transfer shaft 2
- $i_{f2}$  = final reduction gear ratio 2
- $k_o$  = torsional stiffness of the output shaft, N/rad
- $c_o$  = damping coefficient of the output shaft, N·s/rad
- $T_{c1}$  = clutch 1 torque, N·m
- $T_{c2}$  = clutch 2 torque, N·m
- $T_m$  = torque from power sources, N·m

$T_{cl}$  = vehicle resistance torque, N·m

The driveline model (1) well describes torsional vibrations of the driveshaft that occur during gear shifts of a DCT equipped vehicle. In addition, because it contains the states of clutch slip speed and output shift torque, we can control both the shift speed and smoothness effectively based on this reduced-order model. Note that the states  $\dot{\omega}_1$  and  $\dot{\omega}_2$  are generally considered as control outputs of a gear shifting system, since the states are directly related to the whole shift quality. For more information on the detailed modeling procedure and validation of the model, please see the paper<sup>12</sup>.

## 2 Robust Controller Design

In this paper, we are focusing only on the inertia phase of which control performance mostly determines the total shift quality. As soon as the off-going clutch begins to slip, the inertia phase starts. Thus, it is assumed the off-going clutch (clutch 1) is disengaged during the inertia phase, i.e.  $T_{cl} \approx 0$ . In this subsection, a robust controller is designed to track the reference state trajectories taking into account various model uncertainties and disturbances. The control states are the slip speed of the on-coming clutch (clutch 2) and the output shaft torque, and the torque inputs of the drive motor and the on-coming clutch are regarded as control inputs. Note that in (1), the power source torque stands for the total torque from the engine and the drive motor, i.e.  $T_{in} \approx T_e + T_m$ . Next, a robust multivariable method using H-infinity loop shaping is developed based on the control-oriented model for the gear shift. The design procedure of the controller is two stages: design of the pre-filter to shape the open-loop response of the plant, and robust stabilization of the closed-loop system by solving the H-infinity problem. By considering the vehicle load torque as the disturbance input to the system, the transfer function matrix for the DCT driveline is easily obtained using (1). Assuming the nominal transfer function matrix is denoted as  $G$ , the prefilter  $W$  should be designed so that the singular values of the shaped plant  $G_s = WG$  are properly determined. The detailed design process is specified in<sup>13</sup>. Here, considering the physical characteristics of the actual plant, pure integrators with gain crossover frequencies of 20 rad/s and 10rad/s were chosen as the desired loop shapes for control loops of drive motor and clutch.

Next, it is assumed that the nominal shaped plant  $G_s$  filtered by the prefilter has normalized left coprime factorization as follows<sup>14</sup>:

$$G_s = M^{-1}N. \quad (2)$$

The perturbed shaped plant  $G_{s,p}$  then can be described as:

$$G_{s,p} = \left\{ (M + \Delta_M)^{-1} (N + \Delta_N) : \left\| \begin{bmatrix} \Delta_N & \Delta_M \end{bmatrix} \right\|_{\infty} < \varepsilon \right\} \quad (3)$$

where  $\Delta_N$  and  $\Delta_M$  are stable unknown transfer functions standing for the model uncertainties,  $\|\cdot\|_{\infty}$  represents the H-infinity norm, and  $\varepsilon > 0$  is the stability margin. For the perturbed system, the feedback controller K is robust if and only if the nominal feedback system is stable and

$$\gamma = \left\| \begin{bmatrix} K \\ I \end{bmatrix} (I - G_s K)^{-1} M^{-1} \right\|_{\infty} \leq \frac{1}{\varepsilon}. \quad (4)$$

The optimal (lowest) value of  $\gamma$  and the maximum stability margin  $\varepsilon$  are provided as (5)<sup>14</sup>.

$$\gamma_{\min} = \varepsilon_{\max}^{-1} = \left\{ -\left\| \begin{bmatrix} N & M \end{bmatrix} \right\|_H^2 \right\}^{\frac{1}{2}} = \left(1 + \rho(XZ)\right)^{\frac{1}{2}}, \quad (5)$$

where  $\|\cdot\|_H$  is the Hankel norm and  $\rho$  is the spectral radius.

For the minimal state-space realization  $(A, B, C, D)$  of  $G_s$ ,  $Z$  and  $X$  are the unique positive definite solutions to the following two algebraic Riccati equations (6) and (7).

$$(A - BS^{-1}D^T C)Z + Z(A - BS^{-1}D^T C)^T - ZC^T R^{-1} CZ + BS^{-1}B^T = 0 \quad (6)$$

where  $R = I + DD^T$ ,  $S = I + D^T D$  and

$$(A - BS^{-1}D^T C)X + X(A - BS^{-1}D^T C)^T - XBR^{-1}B^T Z + C^T R^{-1} C = 0 \quad (7)$$

Here, the shaped plant (2) for the DCT driveline has  $D \approx 0$ , and eqns (6) and (7) are significantly simplified. Then, the stabilizing controller  $K_s$  for  $G_s$  that guarantees

$$\left\| \begin{bmatrix} K_s \\ I \end{bmatrix} (I - G_s K)^{-1} M^{-1} \right\|_{\infty} \leq \gamma \quad (8)$$

for a specified  $\gamma > \gamma_{\min}$  is derived using the explicit formula specified in <sup>15</sup>. The final H-infinity loop shaping controller is denoted as  $K = WK_s$ . The controller  $K$  generates targeted torque values for the drive motor and the clutch 2 during the inertia phase in real time. Then, the torque command for the clutch is converted into the desired position of the clutch actuator through the experimental map. The motor driver (inverter) automatically controls the motor in accordance with the motor torque command, and the actuator position controller plays a role to control the actuator to track the desired clutch actuator position through a simple PID control law.

### 3 SIMULATIONS

#### 1 Control performance validation

Simulations through a proven SimDriveline powertrain model were conducted to validate the proposed control strategy. The reference trajectories of the control outputs for the inertia phase were given such that the shift shock could be minimized while satisfying the shift time criterion. In specific, the reference shape of the on-coming clutch slip speed was designed such that the magnitude of its deceleration increases during the first half of the inertia phase to reduce the shift time and then decreases until the end of the inertia phase for good shift quality. At the end of the inertia phase, the slip acceleration should be zero to eliminate the torque discontinuity at the clutch lock-up. Also, the output shaft torque values should increase during the first half of the inertia phase for fast engagement and decrease during the other half to minimize the lock-up shock. since a sensor for the output torque is not available in a real vehicle, the torque observer developed in <sup>16</sup> was used for feedback control of the output torque.

The control results were shown in Fig. 4. The slip speed and the output shaft torque tracked the desired values accurately, so the gear shift was completed within the desired time and the driveline oscillations were minimized.

## 2 Robustness analysis

For comparative analysis, another simulation with conventional PD controller was done under the same gear shift scenario. Differently from the proposed robust controller, it is difficult to tune the PD control gains for each control loop independently because of the strong loop interaction. The control gains were tuned repetitively to meet the similar tracking performances as the proposed multivariable control. The results of the PD controller are described in Fig. 5.

Even though the tracking performances of both control methods are comparable, much more time-consuming calibration efforts are required for the decentralized PD control to exhibit the same control performances as the proposed multivariable control. Another advantage of the proposed controller over the conventional PD controller is its robustness to model uncertainties and unknown disturbances. To directly compare the robustness of both controllers, two additional simulations were carried out under the scenario when the feedforward control law is inaccurate; that is, 30% error is intentionally assigned to the original feedforward control. The corresponding results of the proposed controller and the PD controller are shown in Figs. 6 and 7, respectively.

The robust performance of the proposed controller was verified from Fig. 6, since its control performance was not degraded at all even when the feedforward control law was very inaccurate. However, the inaccurate feedforward control had a direct adverse effect on the PD control performance, as shown in Fig. 7. Since the feedforward control law had 30% uncertainty (70% of the original feedforward term in magnitude), the similar amount of the tracking error occurred in the control response of the output shaft torque. The only way to recover the control performance the same as the results of Fig. 6 is to re-tune the control gains, which is very time-consuming and undesirable. In results, because of the poor robustness of the conventional controller (Fig. 7(d)), the gear shift was not completed within the desired time (the clutch was still slipping at around 6.2s in Fig. 7(c)).

In order to demonstrate the robust properties of both controllers effectively, the clutch torque input values, (denoted as  $T_{c2,d}$ ) corresponding to Figs. 6-7 are plotted as follows. In Fig.8, when there was some error in the feedforward control law, the proposed controller automatically corrected the feedback control efforts to maintain the whole control performance, which indicated the robustness of the proposed controller. On the other hand, in the case of the conventional PD controller, there was not much change in the feedback control in the presence of the inaccurate feedforward control law, which led to the poor control results in Fig. 9. In results, it was observed from Figs. 6-9 that the proposed controller is robust to the model uncertainty (inaccurate feedforward control), compared with the conventional PD controller.

## 4 CONCLUSION

In this paper, a robust controller is designed to effectively handle the model uncertainties and disturbances during the gear shift of the HEV with DCT. The feasibility of the robust control scheme was demonstrated through various simulations, and its robustness against the model uncertainties was also proved by the comparative studies. The results indicated that the proposed robust torque control strategy significantly improved the shift performance of the HEV with DCT. Using the robust control scheme, the speed state as well as the torque state tracked the reference trajectories with precision even in the presence of model uncertainties, which resulted in smooth and fast shift responses. Future works

should focus on further simplification of the proposed control scheme in order to increase the applicability to actual vehicles.

## 5 ACKNOWLEDGMENTS

This manuscript is an extended version of the original presentation made at MOVIC 2018 (the 14<sup>th</sup> International Conference on Motion and Vibration Control), Daejeon, Aug. 2018.

## 6. REFERENCES

1. P. Pisu and G. Rizzoni, "A comparative study of supervisory control strategies for hybrid electric vehicles," *IEEE Transactions on Control Systems Technology*, vol. 15, pp. 506-518, 2007.
2. D. Kum, H. Peng, and N. K. Bucknor, "Supervisory control of parallel hybrid electric vehicles for fuel and emission reduction," *Journal of dynamic systems, measurement, and control*, vol. 133, p.061010, 2011.
3. C.-C. Lin, H. Peng, J. W. Grizzle, and J.-M. Kang, "Power management strategy for a parallel hybrid electric truck," *IEEE transactions on control systems technology*, vol. 11, pp. 839-849, 2003.
4. E. Galvagno, M. Velardocchia, and A. Vigliani, "Dynamic and kinematic model of a dual clutch transmission," *Mechanism and Machine Theory*, vol. 46, pp. 794-805, 2011.
5. J. Kim, S. B. Choi, and J. J. Oh, "Adaptive Engagement Control of a Self-Energizing Clutch Actuator System Based on Robust Position Tracking," *IEEE/ASME Transactions on Mechatronics*, vol. 23, pp.800-810, 2018.
6. K. van Berkel, T. Hofman, A. Serrarens, and M. Steinbuch, "Fast and smooth clutch engagement control for dual-clutch transmissions," *Control Engineering Practice*, vol. 22, pp. 57-68, 2014.
7. Y. Liu, D. Qin, H. Jiang, and Y. Zhang, "Shift control strategy and experimental validation for dry dual clutch transmissions," *Mechanism and Machine Theory*, vol. 75, pp. 41-53, 2014.
8. P. D. Walker, N. Zhang, and R. Tamba, "Control of gear shifts in dual clutch transmission powertrains," *Mechanical Systems and Signal Processing*, vol. 25, pp. 1923-1936, 2011.
9. S. Kim, J. Oh, and S. Choi, "Gear shift control of a dual-clutch transmission using optimal control allocation," *Mechanism and Machine Theory*, vol. 113, pp. 109-125, 2017.
10. B. Z. Gao, H. Chen, K. Sanada, and Y. Hu, "Design of clutch-slip controller for automatic transmission using backstepping," *Mechatronics, IEEE/ASME Transactions on*, vol. 16, pp. 498-508, 2011.
11. F. Meng, G. Tao, T. Zhang, Y. Hu, and P. Geng, "Optimal shifting control strategy in inertia phase of an automatic transmission for automotive applications," *Mechanical Systems and Signal Processing*, vol. 60, pp. 742-752, 2015
12. S. Kim and S. Choi, "Control-oriented modeling and torque estimations for vehicle driveline with dual-clutch transmission," *Mechanism and Machine Theory*, vol. 121, pp. 633-649, 2018.
13. V. Le and M. Safonov, "Rational matrix GCDs and the design of squaring-down compensators-a state-space theory," *IEEE Transactions on Automatic Control*, vol. 37, pp. 384-392, 1992.
14. S. Skogestad and I. Postlethwaite, *Multivariable feedback control: analysis and design vol. 2*: Wiley New York, 2007.

15. K. Glover and D. McFarlane, "Robust stabilization of normalized coprime factor plant descriptions with  $H_{\infty}$ -bounded uncertainty," IEEE transactions on automatic control, vol. 34, pp. 821-830, 1989.
16. S. Kim, J. J. Oh, and S. B. Choi, "Driveline Torque Estimations for a Ground Vehicle with Dual-clutch Transmission," IEEE Transactions on Vehicular Technology, vol. 67, pp. 1977-1989, 2018.
17. S. Kim and S. B. Choi. "Cooperative Control of Drive Motor and Clutch for Gear Shift of Hybrid Electric Vehicles with Dual-clutch Transmission." IEEE/ASME Transactions on Mechatronics, vol. 25, pp. 1578-1588, 2020.

### List of Figure Captions

*Fig. 1— Structure of a HEV with DCT.*

*Fig. 2— Schematic of a simplified driveline model for a HEV with DCT.*

*Fig. 3— Robust stabilizing control structure.*

*Fig. 4— Simulation results of the proposed control method: (a) clutch actuator positions, (b) torques (c) angular speeds, (d) slip speed of on-coming clutch, (e) output shaft torque, (f) vehicle jerk.*

*Fig. 5— Simulation results of conventional PD control: (a) clutch actuator positions, (b) torques (c) angular speeds, (d) slip speed of on-coming clutch, (e) output shaft torque, (f) vehicle jerk.*

*Fig. 6— Results of the proposed controller when the feedforward control law is inaccurate (30% error): (a) torques (b) angular speeds, (c) slip speed of on-coming clutch, (d) output shaft torque.*

*Fig. 7— Results of the PD controller when the feedforward control law is inaccurate (30% error): (a) torques (b) angular speeds, (c) slip speed of on-coming clutch, (d) output shaft torque.*

*Fig. 8— Robustness analysis of the proposed controller: (a) when no feedforward control uncertainty exists, (b) when 30% error of feedforward control exists.*

*Fig. 9— Robustness analysis of the PD controller: (a) when no feedforward control uncertainty exists, (b) when 30% error of feedforward control exists.*



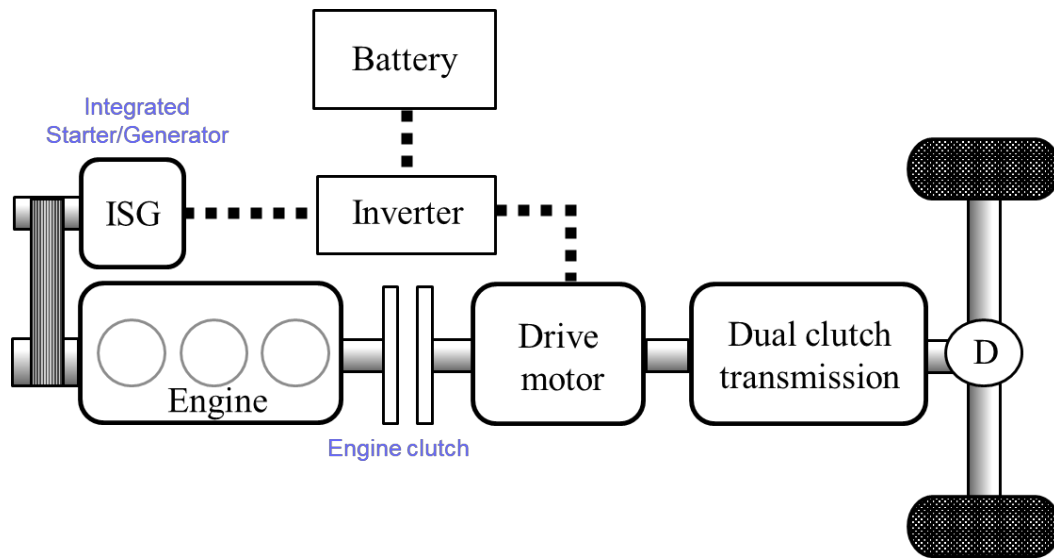


*Fig. 1— Structure of a HEV with DCT.*

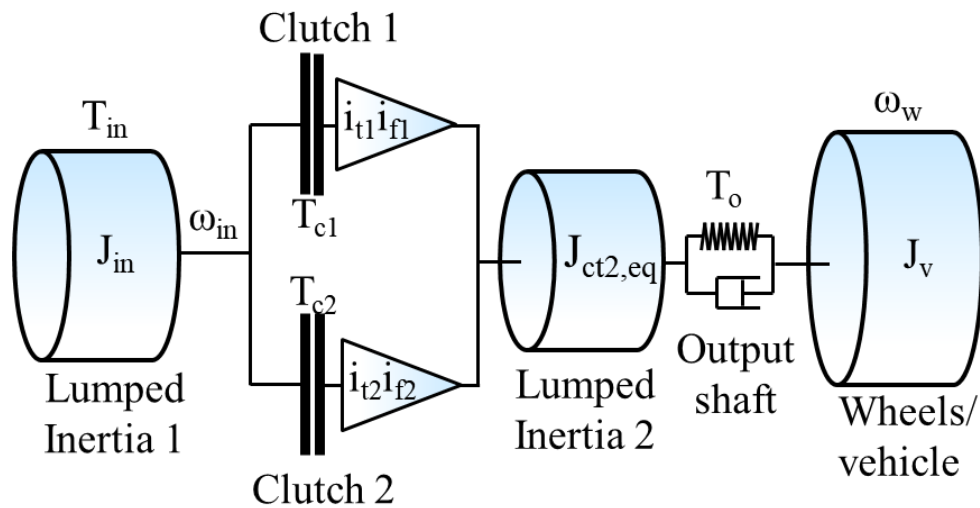
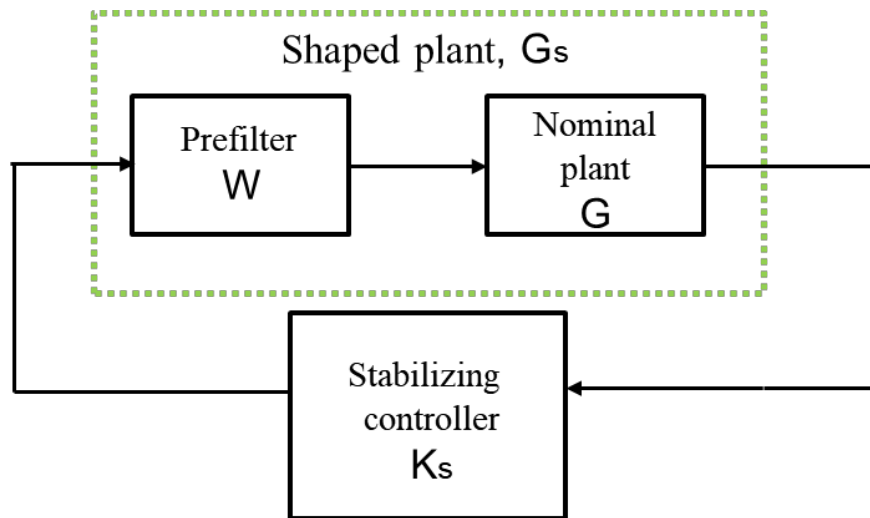
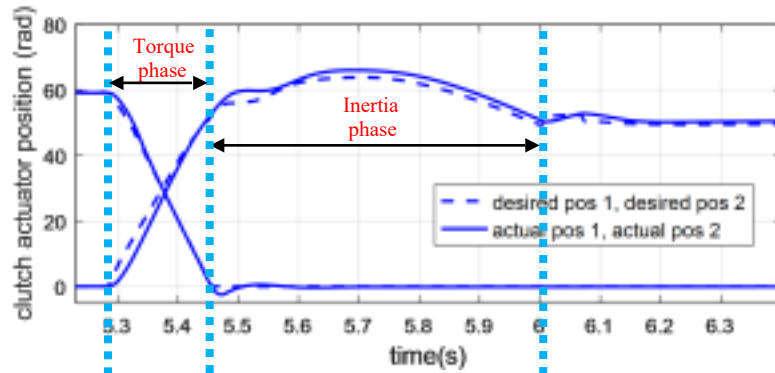


Fig. 2— Schematic of a simplified driveline model for a HEV with DCT.

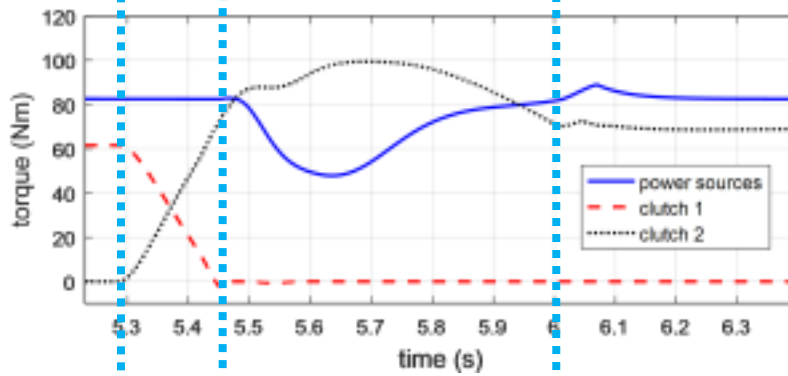
- $T_{c1}$  : Clutch 1 torque,
- $T_{c2}$  : Clutch 2 torque,
- $T_{in}$  : Torque from power sources,
- $T_o$  : Output shaft torque,
- $\omega_{in}$  : Speed of power sources (for parallel mode operation),
- $\omega_w$  : Wheel speed.)



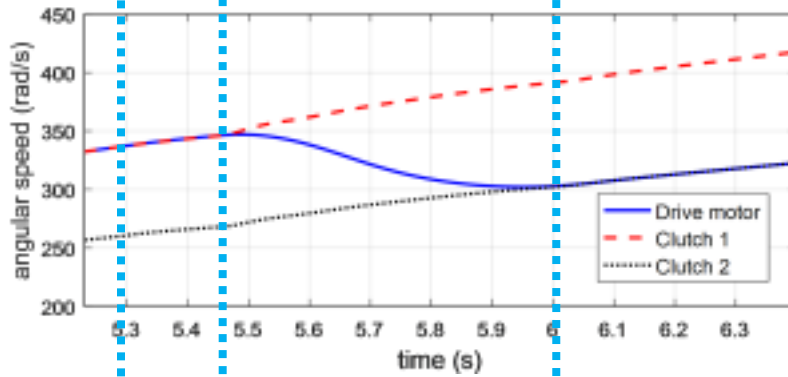
*Fig. 3—* Robust stabilizing control structure.



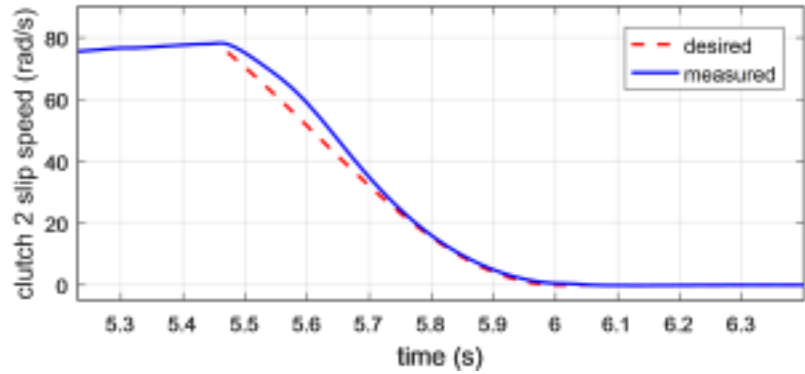
(a)



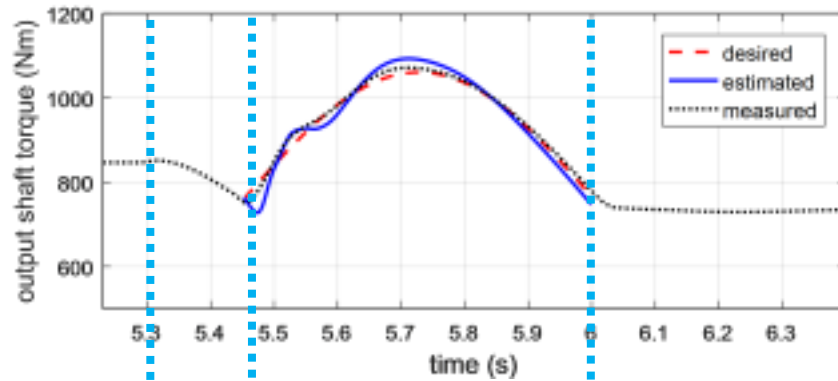
(b)



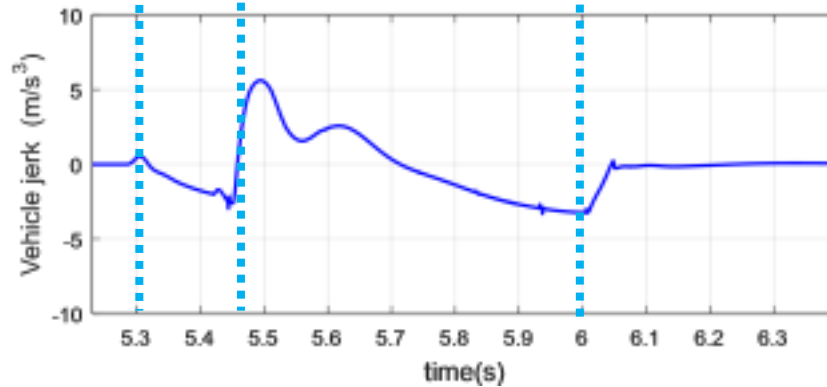
(c)



(d)

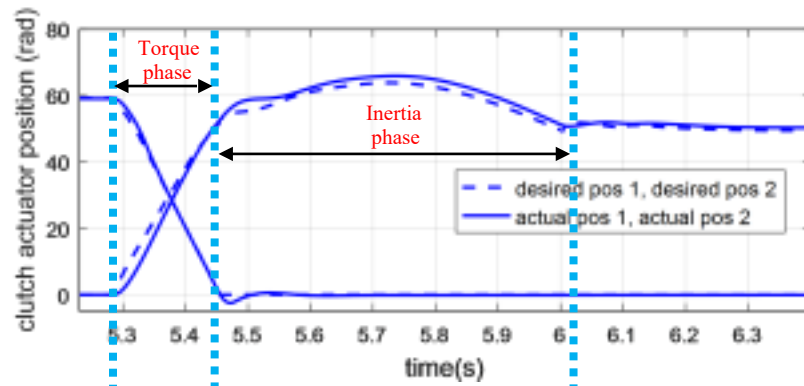


(e)

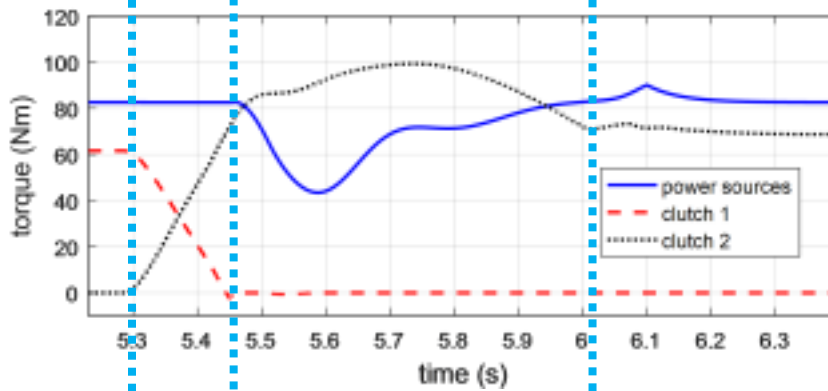


(f)

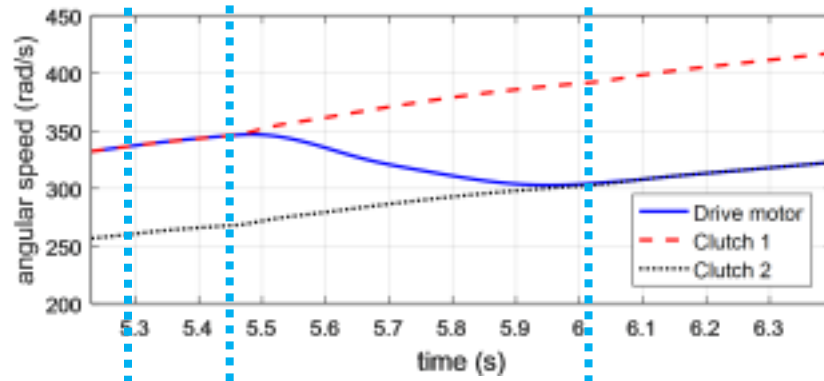
*Fig. 4*— Simulation results of the proposed control method: (a) clutch actuator positions, (b) torques (c) angular speeds, (d) slip speed of on-coming clutch, (e) output shaft torque, (f) vehicle jerk



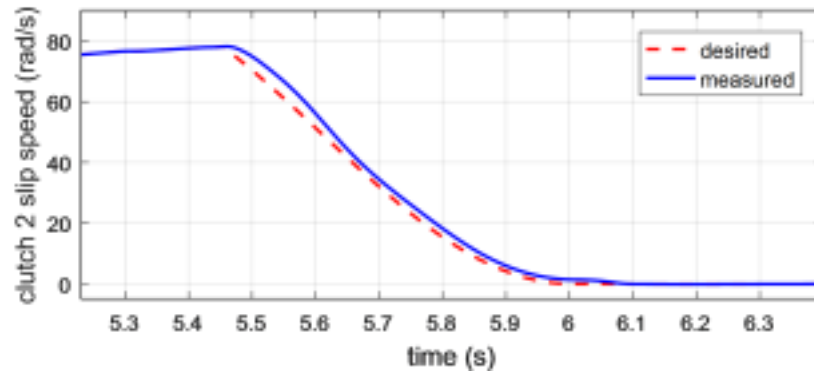
(a)



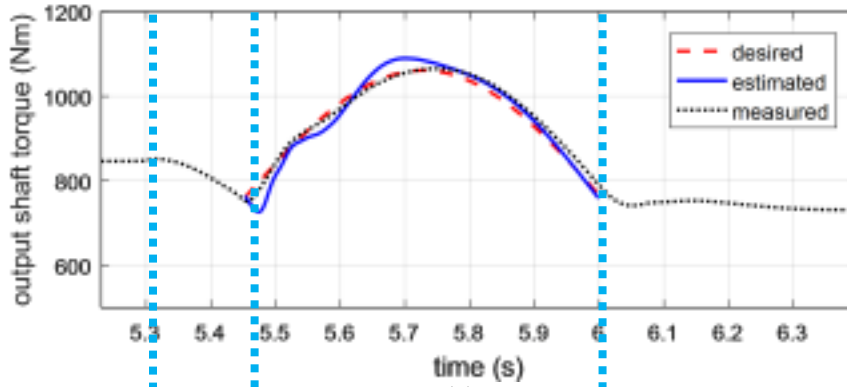
(b)



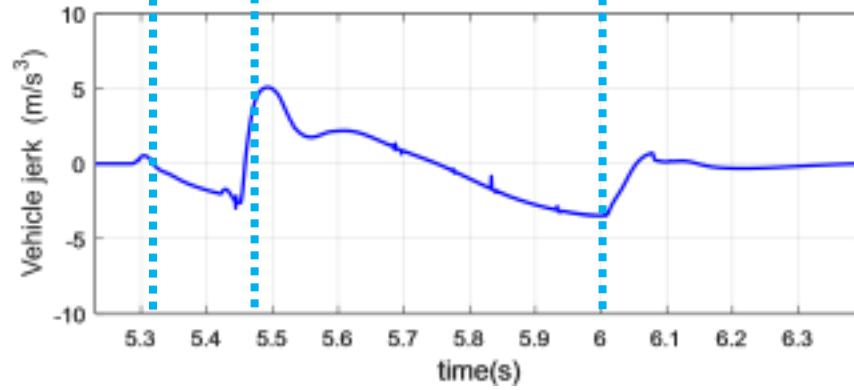
(c)



(d)

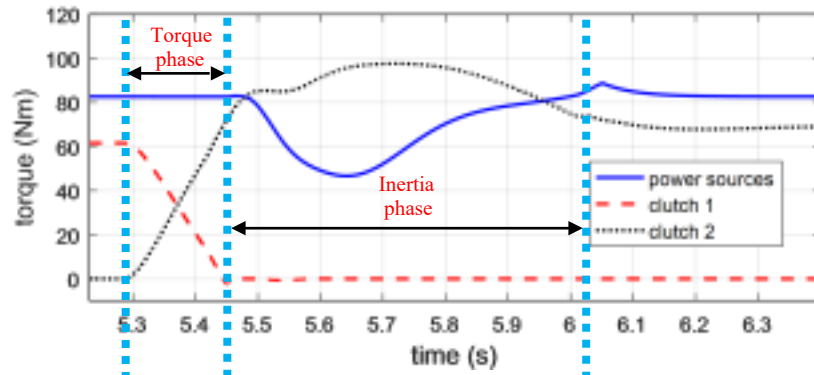


(e)

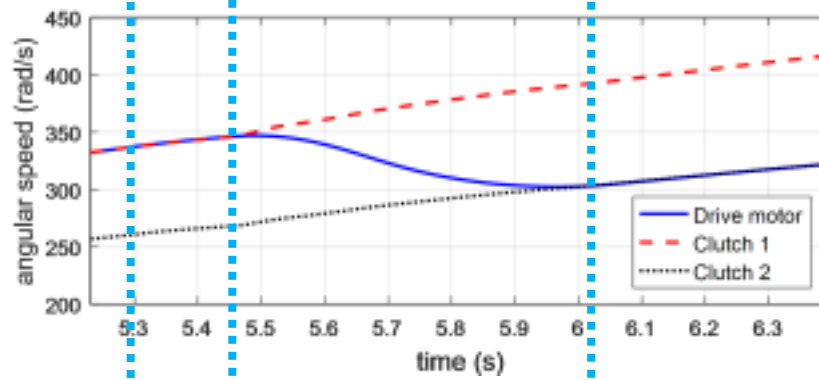


(f)

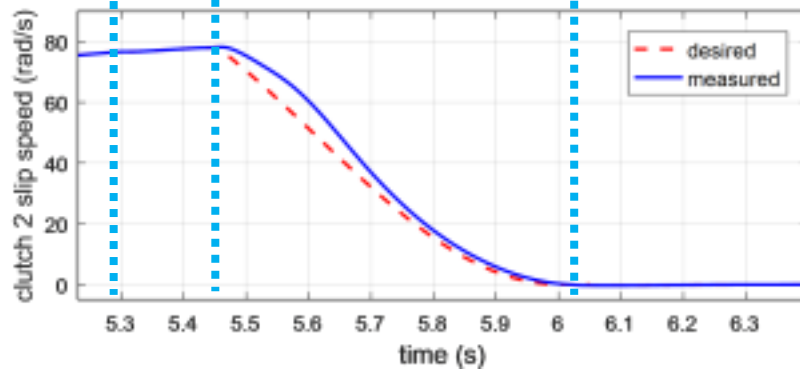
Fig. 5— Simulation results of conventional PD control: (a) clutch actuator positions, (b) torques (c) angular speeds, (d) slip speed of on-coming clutch, (e) output shaft torque, (f) vehicle jerk.



(a)

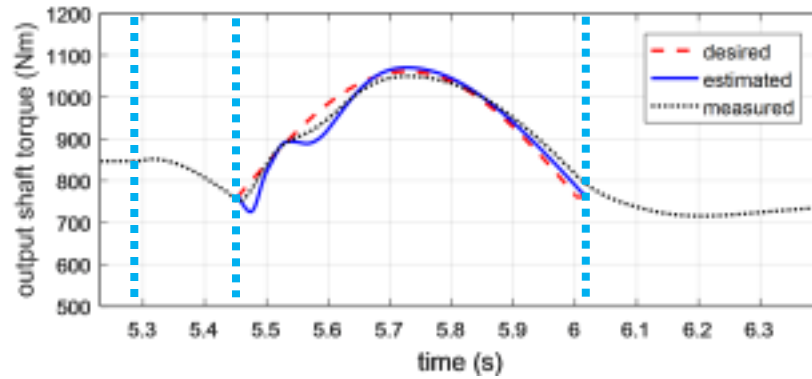


(b)



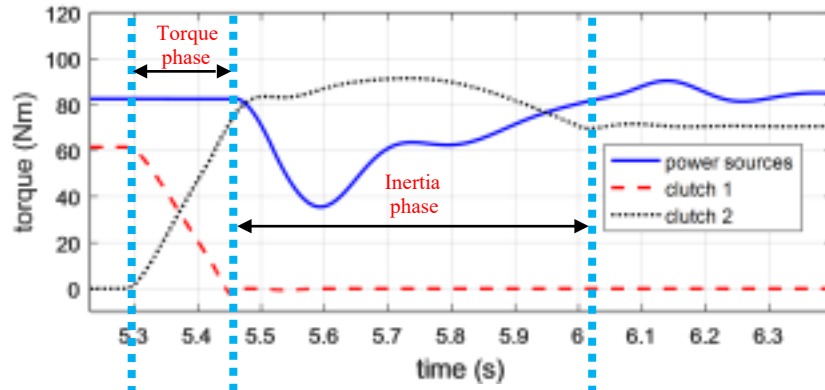
(c)



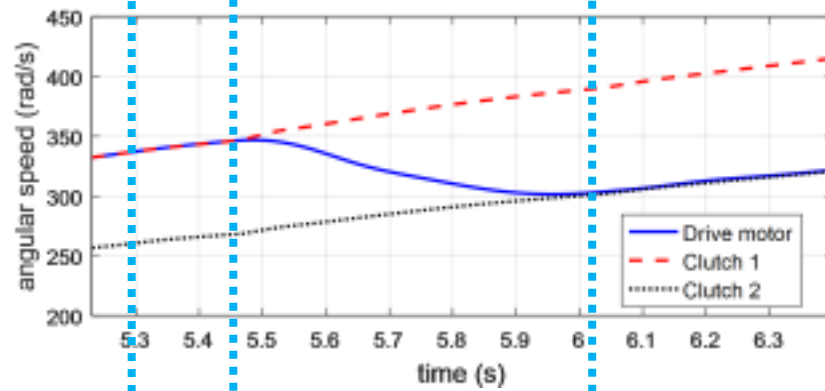


(d)

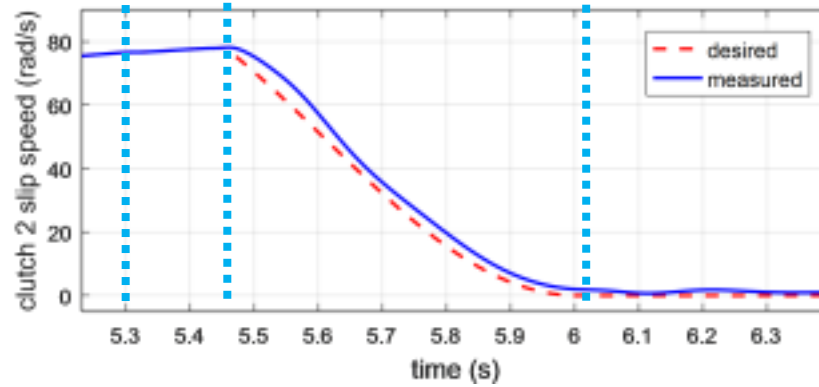
*Fig. 6*— Results of the proposed controller when the feedforward control law is inaccurate (30% error): (a) torques (b) angular speeds, (c) slip speed of on-coming clutch, (d) output shaft torque.



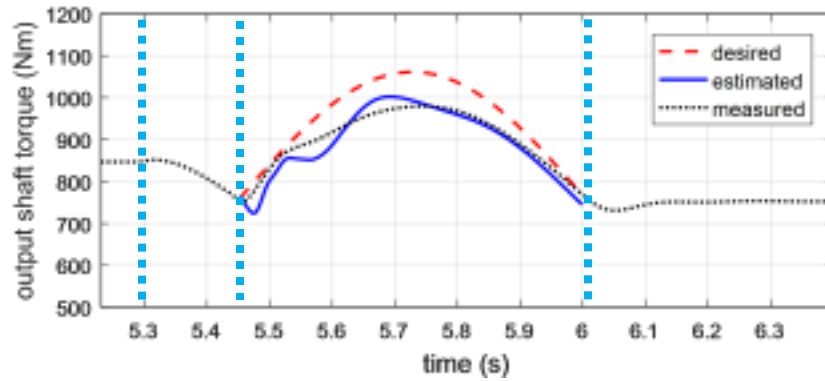
(a)



(b)



(c)



(d)

Fig. 7— Results of the PD controller when the feedforward control law is inaccurate (30% error): (a) torques (b) angular speeds, (c) slip speed of on-coming clutch, (d) output shaft torque.

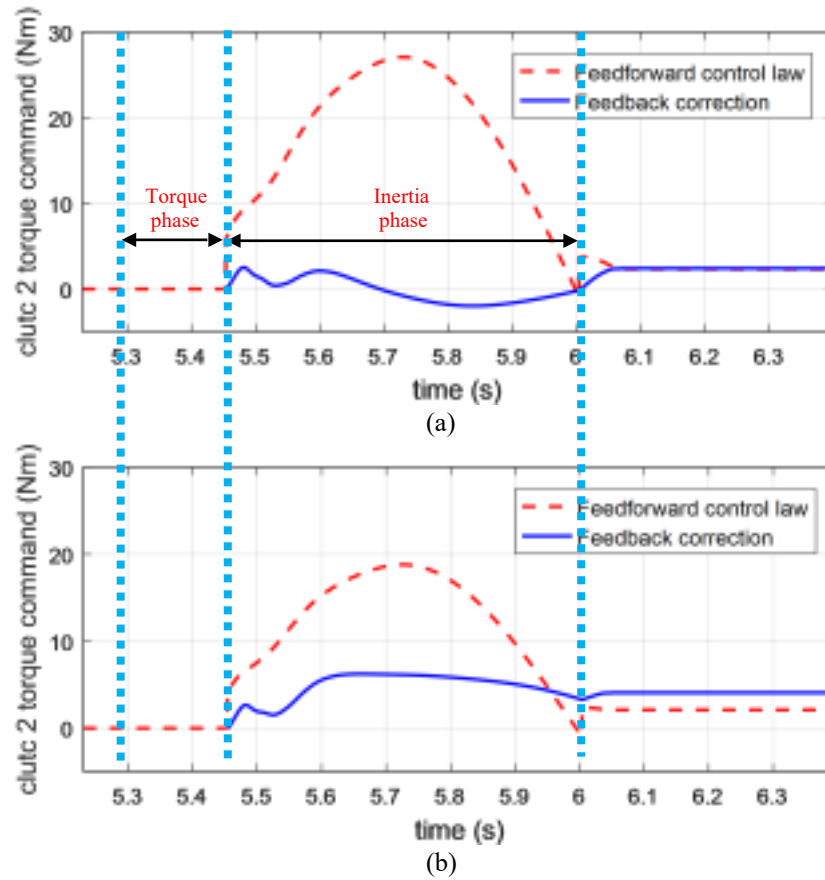


*Fig. 8*— Robustness analysis of the proposed controller: (a) when no feedforward control uncertainty exists, (b) when 30% error of feedforward control exists.

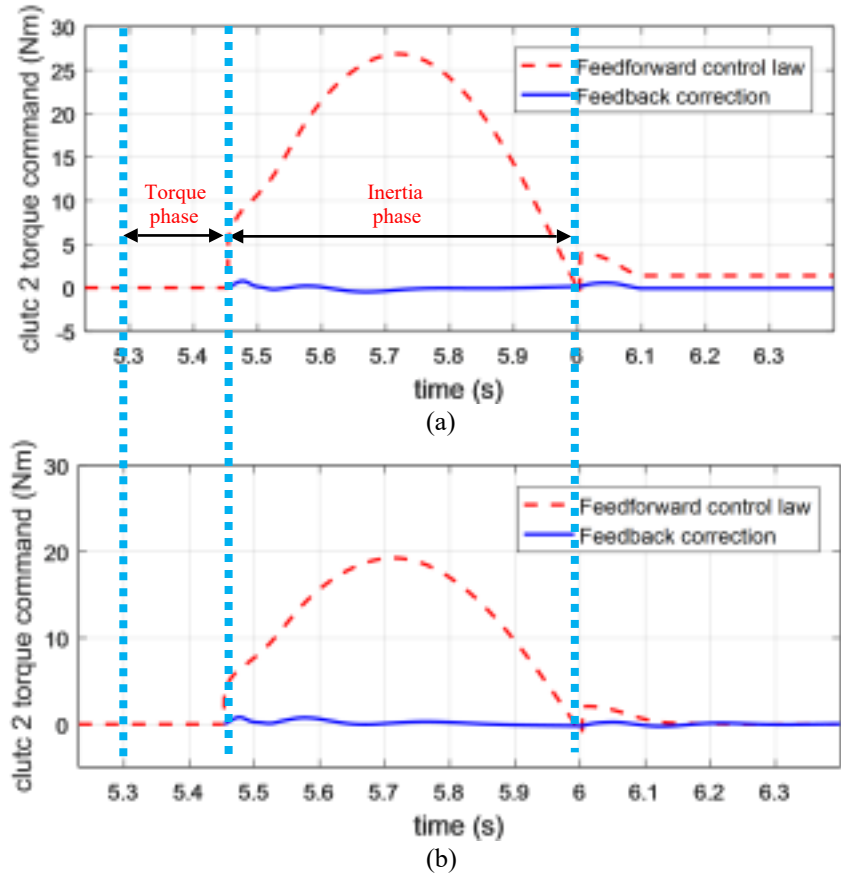


Fig. 9— Robustness analysis of the PD controller: (a) when no feedforward control uncertainty exists, (b) when 30% error of feedforward control exists.